Carbohydrate Research 401 (2015) 115–121

Contents lists available at ScienceDirect

Carbohydrate Research

journal homepage: www.elsevier.com/locate/carres

α-Galactobiosyl units: thermodynamics and kinetics of their formation by transglycosylations catalysed by the GH36 α-galactosidase from *Thermotoga maritima*

Anna S. Borisova [a,b], Dina R. Ivanen [a], Kirill S. Bobrov [a], Elena V. Eneyskaya [a], Georgy N. Rychkov [a,c], Mats Sandgren [b], Anna A. Kulminskaya [a,c,*], Michael L. Sinnott [d], Konstantin A. Shabalin [a,c]

[a] National Research Center "Kurchatov Institute", B.P. Konstantinov Petersburg Nuclear Physics Institute, Orlova Roscha, 188300 Gatchina, Russia
[b] Department of Chemistry and Biotechnology, Swedish University of Agricultural Sciences, Uppsala, Sweden
[c] St. Petersburg State Polytechnical University, 29 Politechnicheskaya str., 195251 St. Petersburg, Russia
[d] Department of Chemical Sciences, University of Huddersfield, Queensgate, Huddersfield HD1 3DH, UK

ARTICLE INFO

Article history:
Received 30 April 2014
Received in revised form 6 November 2014
Accepted 8 November 2014
Available online 21 November 2014

Keywords:
α-Galactosidase
Thermotoga maritima
Regioselectivity
Transglycosylation
Kinetics
Free energy differences

ABSTRACT

Broad regioselectivity of α-galactosidase from *Thermotoga maritima* (*Tm*Gal36A) is a limiting factor for application of the enzyme in the directed synthesis of oligogalactosides. However, this property can be used as a convenient tool in studies of thermodynamics of a glycosidic bond. Here, a novel approach to energy difference estimation is suggested. Both transglycosylation and hydrolysis of three types of galactosidic linkages were investigated using total kinetics of formation and hydrolysis of *p*NP-galactobiosides catalysed by monomeric glycoside hydrolase family 36 α-galactosidase from *T. maritima*, a retaining *exo*-acting glycoside hydrolase. We have estimated transition state free energy differences between the 1,2- and 1,3-linkage ($\Delta\Delta G^{\ddagger}_0$ values were equal 5.34 ± 0.85 kJ/mol) and between 1,6-linkage and 1,3-linkage ($\Delta\Delta G^{\ddagger}_0$ = 1.46 ± 0.23 kJ/mol) in *p*NP-galactobiosides over the course of the reaction catalysed by *Tm*Gal36A. Using the free energy difference for formation and hydrolysis of glycosidic linkages ($\Delta\Delta G^{\ddagger}_F - \Delta\Delta G^{\ddagger}_H$), we found that the 1,2-linkage was 2.93 ± 0.47 kJ/mol higher in free energy than the 1,3-linkage, and the 1,6-linkage 4.44 ± 0.71 kJ/mol lower.

© 2014 Elsevier Ltd. All rights reserved.

1. Introduction

In nature, the diversity of glycosidic linkages enables carbohydrate structures to have various functions. Synthesis of different oligosaccharides is required due to varied purposes. Transglycosylation by wild-type retaining glycoside hydrolases still has its place in the glycobiologist's armamentarium, as the disadvantages of alternative technique remain numerous.[1] Fully chemical synthesis, with its cycles of protection and deprotection, requires all the labour of an initial synthesis to be repeated for each subsequent one, and on a large scale, toxic waste becomes problematic.[2] Enzymic synthesis using glycosyltransferases and nucleotide sugar donors becomes prohibitively expensive unless elaborate cycles for donor regeneration are devised.[3] Glycosynthases (retaining glycosidases in which the enzyme nucleophile has typically been mutated to serine)[4,5] require a heavy initial investment in molecular biology with no absolute guarantee of success and glycosyl fluoride substrates of opposite anomeric configuration to the natural substrates. Wild-type retaining glycosidases thus have their place in the synthesis of intrasaccharide linkages. To be useful in saccharide synthesis, they should be thermally stable and have a well-defined +1 site. Subsequent hydrolysis of the product competes with transformation of the glycosyl donor, so donors with particularly high k_{cat}/K_m values should be accessible and stable.

A common problem for glycoside hydrolases is their wide regioselectivity, which results in a number of products with a range of linkages. Nevertheless, a number of α-galactosidases have been studied for their ability to synthesize various oligogalactosides.[6–10] To the best of our knowledge, no comparative studies have been reported on regioselectivity of α-galactosidases in the

Abbreviations: *Tm*Gal36A, α galactosidase from *Thermotoga maritima*; *p*NP, *para*-nitrophenol; *p*NPGal, *p*NP-α-D-galactopyranoside; 1,2diGal, α-D-Gal*p*-(1 → 2)-α-D-Gal*p*; 1,3diGal, α-D-Gal*p*-(1 → 3)-α-D-Gal*p*; 1,4diGal, α-D-Gal*p*-(1 → 4)-α-D-Gal*p*; 1,6diGal, α-D-Gal*p*-(1 → 6)-α-D-Gal*p*; *p*NP1,2diGal, α-D-Gal*p*-(1 → 2)-α-D-Gal*p*-*O*-*p*NP; *p*NP1,3diGal, α-D-Gal*p*-(1 → 3)-α-D-Gal*p*-*O*-*p*NP; *p*NP1,6diGal, α-D-Gal*p*-(1 → 6)-α-D-Gal*p*-*O*-*p*NP; *p*NPdiGal, *p*NP-digalactopyranoside.

* Corresponding author. Tel./fax: +7 81371 32014.
E-mail address: kulm@omrb.pnpi.spb.ru (A.A. Kulminskaya).

http://dx.doi.org/10.1016/j.carres.2014.11.003
0008-6215/© 2014 Elsevier Ltd. All rights reserved.

hydrolysis and synthesis of oligogalactosides with all possible linkages, particularly within the context of determining the relative thermodynamic stability of the products.

Traditionally, the thermodynamics of glycosidic linkages have been analysed via hydrolysis reactions, calorimetry yielding change in enthalpy, ΔH^0 and measurements of positions of hydrolytic equilibrium giving change in Gibbs free energy, ΔG°. Some early papers report differences between the hydrolysis enthalpies of α-1,4- and α-1,6-glycosidic linkages,[11,12] and more detailed studies of different oligosaccharide hydrolyses enabled both enthalpy and entropy changes to be measured.[13] In the present paper, a novel approach to estimation of free energy differences is suggested. Both transglycosylation and hydrolysis of three types of α-galactosidic linkages were investigated using total kinetics of formation and hydrolysis of *p*NP-galactobiosides catalysed by monomeric glycoside hydrolase family 36 (GH36) α-galactosidase from *Thermotoga maritima*, a retaining exo-acting glycoside hydrolase.[14] Both enzymatically and chemically synthesized substrates were used for the complete analysis of regioselectivity and thermodynamics of galactosidic bonds.

2. Results and discussion

2.1. Theoretical background

In the well established chemical mechanism,[15] the nucleophile of the α-galactosidase of *Thermotoga maritima* (GH family 36 in CAZy; PDB code 1ZY9) has been identified as Asp 327 based on the ability of the normally inactive Asp327Gly mutant to convert *p*-nitrophenyl α-galactopyranoside (*p*NPαGal) and azide ion to *p*NP and β-D-galactopyranosyl azide (βGalN_3), as addition of azide ions replaced the excised CH_2COO- grouping. Likewise, the acid-base catalyst was identified as Asp387 from the ability of the Asp387Gly mutant to generate αGalN_3 from *p*NPαGal and azide ion. The β-galactosyl-enzyme intermediate was hydrolytically stable as a result of the absence of general base catalysis but could be directly attacked by azide ion. The available X-ray structure suggests an *anti*-protonation trajectory, and a possible role for Asp 220 in stabilizing oxocarbenium-ion-like transition states.[14]

The minimal kinetic scheme for a retaining glycosidase also acting as a transglycosylase is given by Scheme 1:

Here *E* is the enzyme, *Tm*Gal36A, *S* is *p*NPGal, *E.S* is the Michaelis complex of enzyme and *p*NPGal, *EβGal* is the β-galactosyl-enzyme covalent intermediate and αGalOR_i is a *p*NPdiGal regioisomer. The index *i* (for α-1,2-, α-1,3- and α-1,6-isomers *i* = 1, 2 and 3, respectively) enables the three pathways for hydrolysis and formation of different isomers to be included in brackets on the left-hand side of Scheme 1. *E.*X_i is *E.p*NPdiGal Michaelis complex for the hydrolysis of a *p*NPdiGal regioisomer or is *EβGal.p*NPGal Michaelis complex for the *i*-isomer formation; *E.αGal* is a complex of the enzyme with a product.

When acting as a hydrolase, the Michaelis–Menten parameters are given by $k_{cat} = k_2k_3/(k_2 + k_3)$ and $K_m = k_3(k_1 + k_2)/k_1(k_2 + k_3)$, so that the bimolecular rate constant $k_{cat}/K_m = k_1k_2/(k_{-1} + k_2)$

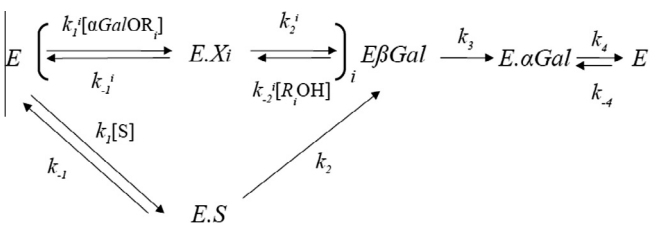

Scheme 1.

contains no terms for processes occurring after galactosyl-enzyme formation. Product inhibition affects the distribution of the different enzyme forms, and thus, influences the absolute rate of hydrolysis and transglycosylation at different times, so the product complex *E.αGal* needs to be included in Scheme 1 for kinetic measurements other than those of initial rates.

In the presence of acceptors R_iOH, which do not have a binding site, the transglycosylation reaction is described by a bimolecular rate constant k_F (see an expression for the constant below), and k_3 in the expressions for k_{cat} and K_m can be replaced by $(k_3 + k_F[R_iOH])$. When the acceptor has a binding site, the possibility that the *EβGal.*R_iOH complex may be in a steady state makes the expressions very complex, although if there is no hydrolysis ($k_3 = 0$), the kinetic analysis simplifies to that of a ping-pong reaction, with A = α*GalO*R, B = R_iOH (see Eq. (1)):

$$V = V_{max}[A][B]/(K_m^B[A] + K_m^A[B] + [A][B]) \quad (1)$$

When $[A] \gg K_m^A$ and $B \ll K_m^B$ the physical situation corresponds to the interception of the galactosyl-enzyme by small concentrations of R_iOH, described either by $k_F[E]_0$ [R_iOH] of the Scheme 1 or $V_{max}[B]/K_m^B$ of the ping-pong mechanism, which are thus seen to be equivalent.

A frequently ignored determinant of regioselectivity is the relative thermodynamic stability of the products.[16] The kinetic parameters for the hydrolysis of a link are related to the kinetics of its formation and its thermodynamic stability by Haldane relationships: those for a classic ping-pong reaction (equivalent to transglycosylation without hydrolysis in the present system) have been explicitly derived.[17] The more complex purely algebraic analysis of a transglycosylation with accompanying hydrolysis, both of *EβGal* and of *EβGal.pNPGal* complex, is not essential for our purposes, since the equations we wish to use to determine regioisomer free energy differences become apparent from inspection of the relevant free energy profiles (reaction coordinate diagrams, Fig. 1).

Figure 1A shows the first half of the profile, explicitly accounting for the generation of the glycosyl-enzyme with all the known or suspected intermediates. However, the important free energy differences are those between the highest transition state and the free enzyme and substrate on one side (given by $k_H = k_{cat}/K_m$ for hydrolysis of α*GalO*R_1) and between the highest transition state and the galactosyl-enzyme (given by k_F) on the other. However, Figure 1B shows that any number of these half-profiles can be fitted together at the galactosyl-enzyme to generate the free energy differences between galactosides (pathways to hydrolysis do not affect free energy differences between glycosides).

Inspection of Fig 1B reveals that the free energy difference between *Gal*OR_2 and *Gal*OR_1 is given by Eq. (2):

$$\Delta G^0_{(1\to 2)} = -RT \ln\left\{k_H^1 k_F^2/(k_F^1 k_H^2)\right\} \quad (2)$$

However, k_F values are equivalent to $(k_{cat}/K_m)^B$ values in a ping-pong mechanism. It is axiomatic in enzyme kinetics that in any situation representing a competition — whether different between different sites in the same molecule or between different molecules—the selectivity observed at any substrate concentration is that dictated by the ratio of k_{cat}/K_m values.[18] Therefore, the ratio k_F^1/k_F^2 can be obtained by measuring the initial ratio of galactoside regioisomers produced from *EβGal* at any concentration. It should be noted that in the present scheme, the galactosyl-enzyme complex *EβGal* is the key component since both hydrolysis and transglycosylation pass *via* its formation.

Second order constants were derived from the Scheme 1 as $k_H^i = k_1^i k_2^i/(k_{-1}^i + k_{-2}^i)$ and $k_F^i = k_{-1}^i k_{-2}^i/(k_{-1}^i + k_{-2}^i)$. Here, k_H^i (equal to k_{cat}/K_m) and k_F^i are second order rate constants for a *p*NPdiGal regioisomer hydrolysis and formation.

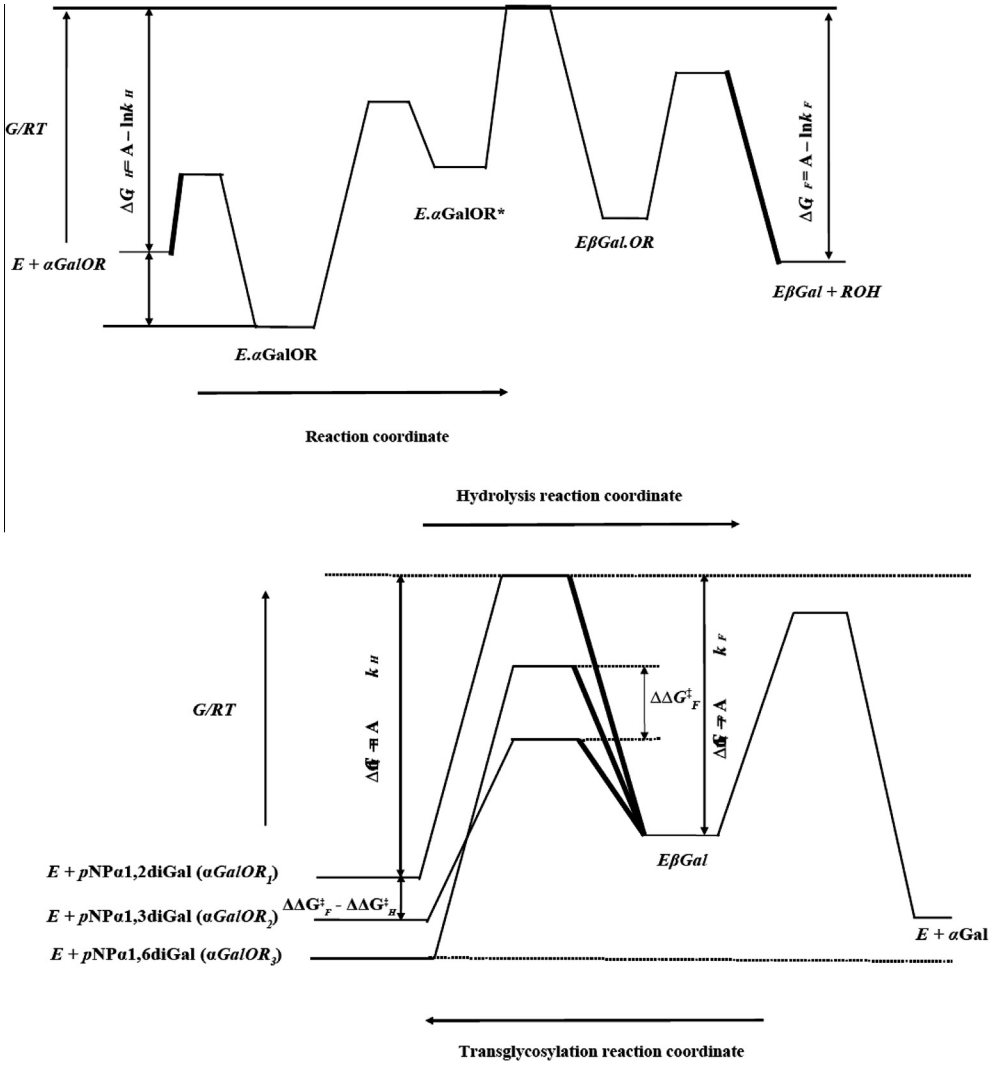

Figure 1. Free energy profiles of the *p*NP digalactosides formation/hydrolysis reaction by *Tm*Gal36A. A: Free energy profile of the half-reaction of a transglycosylating GH36 α-galactosidase, showing intermediates known or suspected: *E.αGal*OR, the Michaelis complex; *E.αGal*OR*, a possible second Michaelis complex suggested on the basis of a low $\beta_{lg}(V/K)$ for aryl galactosides and the possibility of a rate-determining conformation change; *EβGal.*HOR, non-covalent complex of the glycosyl acceptor and leaving group. The existence or otherwise of various complexes interconverted by unimolecular processes does not affect the argument about free energy differences between glycosides, which is based only on second-order rate constants $k_H = k_{cat}/K_m$ and k_F, the rate of reaction of the glycosyl-enzyme with ROH, and the existence of the glycosyl-enzyme. $A = \ln(kT/h)$, where k is Boltzmann's constant, T is the absolute temperature and h is Planck's constant. B: Schematic free energy profiles showing transglycosylations and hydrolysis going through a common galactosyl-enzyme intermediate. Only bimolecular energy barriers, which are rate limiting at low substrate concentrations, are shown. As indicated by the half profile coming above, any number of transglycosylations can be considered, provided the profiles intersect at *E.βGal*.

2.2. Determination of thermodynamics of a galactosidic linkage using transglycosylation

To test these ideas, we carried out several experiments monitoring the formation of transglycosylation products in situ at different substrate concentrations by NMR spectroscopy. At 100 mM-substrate concentration, time-courses for appearance and disappearance of transglycosylation products are typically bell-shaped (Fig. 2). The rate of transglycosylation determines the left-hand part of the curve, while the rate of the hydrolysis of each isomer influences the right branch. The shape of this curve enabled determination of the second order rate constants for both hydrolysis and transglycosylation reactions after fitting the experimental data. We used the methodology described in the Experimental section and Dynafit software[19] to calculate initial rates for formation (V_F^i) of each regioisomer at two concentrations of the substrate (100 and 200 mM, respectively) at the temperature 50 °C. For *p*NP1,3diGal, V_F^i values were 0.35 ± 0.02 and 0.55 ± 0.03 μM/s; for *p*NP1,6diGal, V_F^i values were 0.28 ± 0.02 and 0.31 ± 0.02 μM/s; and for *p*NP1,2diGal V_F^i values were 0.077 ± 0.005 and 0.075 ± 0.010 μM/s. It appeared that at these particular conditions, *p*NPGal hydrolysis occurred with rates of 30 ± 3 and 35 ± 4 μM/s, respectively. Noticeably, increase of initial concentrations of *p*NPGal from 100 to 200 mM leads to 1.6- and 1.1-fold increase of the relative formation rates for α-1,3- and α-1,6-, respectively, while for α-1,2-isomers the transglycosylation rate remains the same. From this, second order rate constants were calculated (Table 1).

The kinetics of transglycosylation were measured at both 50 and 60 °C at 200 mM of initial concentration of *p*NPGal. Ten degrees increase in temperature increased the initial rate of formation 3.1-fold for α-1,3- and α-1,6-isomers and 4.6-fold for the α-1,2-isomer, while the rate of hydrolysis of *p*NPGal increased only twice (from 35 ± 4 μM/s to 71 ± 5 μM/s) (Table S2 in Supplemental material). Regioselectivity of *Tm*Gal36A in transglycosylation reaction towards *p*NP1,3diGal remained the same under various conditions, described above, although relative yields of isomers depended on temperature and the initial concentration of *p*NPGal.

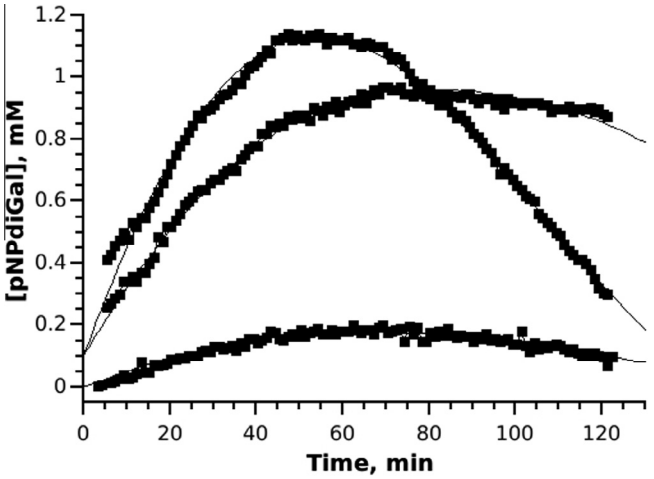

Figure 2. Kinetics of *Tm*Gal36A transglycosylation at 50 °C. The graph represents data obtained at the initial concentration of *p*NPGal equal to 100 mM/L: ● for *p*NP1,3diGal; ♦ for *p*NP1,6diGal; ▲ for *p*NP1,2diGal.

As shown above, one can calculate thermodynamic characteristics, namely the difference between the free energy of the highest transition states for different types of links. For this, constants k_H^i and k_F^i, for example, relative barrier heights $\Delta\Delta G^{\ddagger}_F = RT\ln(k_F^i/k_F^i)$ as well as the free energy differences for different digalactosides (Eq. (2)) can be used. The transition states for formation of the 1,2- and 1,6-isomers can thus be estimated as 5.34 ± 0.85 and 1.46 ± 0.23 kJ/mol higher in free energy than that for the 1,3 isomer (values for Gibbs energy are given for the experimental conditions described in Experimental section).

The ratio of constants k_H^i for different competitive pathways is determined by the free energy difference ($\Delta\Delta G^{\ddagger}_H = RT\ln(k_H^i/k_H^i)$ between their transition states and the starting state (free enzyme and substrate): $\Delta\Delta G^{\ddagger}_H$ values of 2.41 ± 0.39 and 5.90 ± 0.94 kJ/mol have been estimated for the free energy differences between the 1,2- and 1,3-linkage as well as between 1,6-linkage and 1,3-linkage. These free energy differences for formation and hydrolysis of glycosidic linkage ($\Delta\Delta G^{\ddagger}_F - \Delta\Delta G^{\ddagger}_H$) pertain to the *p*-nitrophenyl α-galactobiosides. We found that the 1,2-linkage was 2.93 ± 0.47 kJ/mol higher in free energy than the 1,3-linkage, and the 1,6-linkage 4.44 ± 0.71 kJ/mol lower revealed different stability of each linkage. The free energy difference between more and less stable linkages was 7.37 ± 1.18 kJ/mol and was in line with measurements of hydrolytic equilibrium (e.g., 8.4 kJ/mol difference in free energy of hydrolysis of maltose and isomaltose[17]).

Temperature change had little effect on the free energy difference of the transition state for the 1,6-isomer (−0.2 kJ/mol) but led to 1.2 ± 0.2 kJ/mol decrease in $\Delta\Delta G^{\ddagger}$ for the 1,2-isomer compared to the 1,3-linkage (Table 2). Since $\Delta G = \Delta H - T\Delta S$, that is, varies linearly with temperature, one can estimate a relative impact of enthalpy and entropy into the transition state for both isomers relative to 1,3-isomer. Calculated values for the 1,2-isomer were $\Delta\Delta H^0$ = 45.6 ± 7.3 kJ/mol and $\Delta\Delta S^0$ = −0.12 ± 0.02 kJ/mol/K; for the 1,6-isomer, they were as $\Delta\Delta H^0$ = 8.0 ± 1.3 kJ/mol and $\Delta\Delta S^0$ = −0.020 ± 0.003 kJ/mol/K. Therefore, the relative stabilization of the transition state for the 1,2-linkage in comparison with the 1,3-linkage with increasing temperature was entropy-driven, while for the 1,6-isomer such an effect was minor.

Table 2
Transient state free energy difference relative to 1,3-isomer at two temperatures.

Product	$\Delta\Delta G^{\ddagger}_F$, kJ/M	
	50 °C	60 °C
*p*NP1,2diGal	6.22 ± 1.00	5.00 ± 0.80
*p*NP1,6diGal	1.85 ± 0.30	1.66 ± 0.27

Reactions were carried out at 200 mM initial concentration of the substrate.

2.3. Regioselectivity of *Tm*Gal36A in the hydrolysis of synthetic and natural substrates

Kinetic parameters for *Tm*Gal36A hydrolysis of four chemically synthesized α-galactobioses (1,3diGal, 1,2diGal, 1,6diGal and 1,4diGal) were measured using a Dionex system (Dionex Corporation, USA), in two separate experiments. We observed apparent spontaneous hydrolysis, which was particularly noticeable for 1,3diGal and 1,2diGal, and was likely caused by the highly-alkaline conditions required for analysis of the reaction components by the Dionex equipment, which interfered with measurements of enzymatic hydrolysis. To minimize the effect of spontaneous degradation, the reaction mixture was immediately put on ice and analysed at 10 °C. In order to validate catalytic constants values obtained as described above, relative rates of hydrolysis for each galactobioside were estimated in the experiment with fixed substrate concentration $[S_0] \gg K_m$. The values of k_{cat} were well correlated with the results of this experiment (Table 3).

Additionally, we derived the K_m value for the (UV-silent) galactobiose substrates as the K_I for their inhibition of the hydrolysis of (chromogenic) *p*-nitrophenyl galactoside, since the determination of inhibition constants is very convenient way to estimate the affinity of different substrates. Analysis of the data revealed good agreement between kinetic parameters calculated from different experiments (Table 3). The value for k_{cat}/K_m in hydrolysis of 1,3diGal was 7.8 times higher than that for α-1,2-isomer, 22.3 times higher than for α-1,6-isomer and 776 times higher than for 1,4diGal ($\Delta\Delta G^{\ddagger}_H$ kJ/mol 5.3 ± 0.3, 8.0 ± 0.4 and 17.2 ± 0.9, respectively), and thus *Tm*Gal36A can be considered to have modest regioselectivity towards the α-1,3-linkage in hydrolysis.

For mapping the active site of *Tm*Gal36A, the natural substrates of different lengths (melibiose, α-D-Gal*p*-(1 → 6)-D-Glc*p*; raffinose, α-D-Gal*p*-(1 → 6)-α-D-Glc*p*-(1↔2)-β-D-Fru*f*; and stachyose (α-D-Gal*p*-(1 → 6)-α-D-Gal*p*-(1 → 6)-α-D-Glc*p*-(1↔2)-β-D-Fru*f*) that all contain a fissile α-D-(1 → 6)-Gal*p*-residue were used. According to Hiromi theory,[20] the substrate binding affinity is determined by affinities of sugar residues bound with the glycosidase active site. Usually, a difference of k_{cat} values for oligomeric substrates is due to different quota

Table 1
Second order rate constants for hydrolysis and formation of *p*NPdigalactosides.

Product	k_H^i, 100 mM, 50 °C	k_F^i, 100 mM, 50 °C	k_F^i, 50 °C, 200 mM	k_F^i, 60 °C, 200 mM
*p*NP1,2diGal	37.97 ± 3.04	0.00067 ± 0.00005	0.00073 ± 0.00011	0.00023 ± 0.00003
*p*NP1,3diGal	93.27 ± 7.46	0.00483 ± 0.00039	0.00820 ± 0.00123	0.00143 ± 0.00021
*p*NP1,6diGal	10.37 ± 0.83	0.00280 ± 0.00022	0.00347 ± 0.00052	0.00780 ± 0.00117
*p*NPGal	208.73 ± 16.70	18.33 ± 1.47	18.33 ± 1.47	18.33 ± 1.47

Second order rate constants for hydrolysis were calculated only at 100 mM and 50 °C. Values for k_3 were fixed as 18.33 sec^{-1} (see the Scheme 1). The uncertainties refer to 95% confidence limits.

Table 3
Kinetic parameters of the TmGal hydrolysis of diGals

Substrate	k_{cat}, s^{-1}[a]	Hydrolysis rate[b], s^{-1}	K_m[a], mM	K_i[c], mM	k_{cat}/K_m, s mM^{-1}
1,2diGal	1.4 ± 0.04	0.8 ± 0.02	0.305 ± 0.010	0.42 ± 0.02	4.6 ± 0.2
1,3diGal	2.5 ± 0.08	3.2 ± 0.08	0.07 ± 0.006	0.062 ± 0.008	35.7 ± 1.0
1,4diGal	0.06 ± 0.01	0.04 ± 0.008	1.3 ± 0.05	1.91 ± 0.10	0.046 ± 0.005
1,6diGal	0.16 ± 0.008	0.16 ± 0.01	0.105 ± 0.005	0.11 ± 0.01	1.6 ± 0.1

[a] Values for k_{cat} and K_m were obtained after stopping the reaction by 0.5 M NaOH followed by separation of the reaction products using Dionex system and integration of the corresponding peaks.
[b] Values for hydrolysis rates were derived from the experiments with fixed $[S_0] \gg K_m$. The reaction was stopped by injection of the reaction aliquot onto the column in 0.05 M NaOH, see Section 3.6 of Experimental.
[c] Michaelis constants K_m for galactobiosides were assumed to be equal K_i and calculated from the Dixon plot of reciprocal rates of *p*NPGal hydrolysis ($1/v$) as a function of inhibitor concentration [I].

of productive enzyme-substrate complexes. Kinetic parameters for natural substrate hydrolysis by *Tm*Gal36A are presented in Table 4. The lowest value of K_m, and the highest value of k_{cat}/K_m corresponded for melibiose, with the two other saccharides showing reduced affinity. This suggests the existence of one −1 site and one +1 site in the active centre of *Tm*Gal36A according to the accepted nomenclature.[21]

To illustrate the regioselectivity of *Tm*Gal36A in hydrolysis reactions, flexible docking of natural and synthesized substrates into the active site has been performed, for both anomers of reducing sugars. Melibiose was calculated to bind the most tightly of the α-galactobioses, with the trisaccharide raffinose and the tetrasaccharide stachyose binding less tightly (Table 5), in line with our suggestion of only +1 and −1 subsites in the active site. β-Anomers of reducing sugars were calculated to bind less tightly than α-anomers.

Galactobiosides modelled in the active site represented the same tendency in terms of binding constant resulting in higher affinity for 1,3diGal (Table 3). Affinity of the four different isomers can be ranked in descending order as follows: 1,3diGal, 1,6diGal, 1,2diGal, 1,4diGal, where the lowest and the highest binding constants differed by two orders of magnitude. As shown previously,[22] protein–ligand interactions in situ often have binding energy dominated by such changes in enthalpy and entropy that are not unequivocally predictable, so that each case should be considered individually. It is clearly seen for all the galactobiosides that applying surface energy density constant as low as 0.038 kJ/(mol × Å^2) led to domination of the hydrophobic interactions in total binding free energy. Electrostatic interactions were dominant, likely determining the regioselectivity of the enzyme. According to the docking calculations, an α-1,4-glycosidic bond forced the reducing galactose into an unfavorable conformation in which the plane of the sugar ring rotated along the groove central axis and moved away from the groove bottom (Fig. S1, Supplemental material), which could lead to increase in entropy for this particular galactobioside. This was the only observed conformational change that suggested the mechanism for why cleavage of α-1,4 was slightly disfavored in *Tm*Gal36A hydrolysis and transglycosylation reactions.

Based on the absence of +2 site in *Tm*Gal36A, and neglecting any differential effects of the nitrophenyl group, we hypothesize the same transition states exist in reactions with galactobiosides and *p*NP-galactobiosides. We can calculate that in chromophore-free galactobiosides the 1,2-linkage is 0.48 ± 0.08 kJ/mol lower in free energy than the 1,3-linkage, and the 1,6-linkage 6.47 ± 1.04 kJ/mol lower. Free energy differences for 1,2- and 1,6-linkages in galactobiosides and *p*NP-galactobiosides can be explained by: (a) positioning of the electronegative nitrophenyl-group near the linkage and (b) the increased entropy factor for galactobiosides in the solution resulting in a distribution of furanose and pyranose forms of the terminal galactoside that is essential for the 1,2-linkage (Table S1 in Supplemental material). Thermodynamic reasoning leads to consideration of only three states: a mixture of free enzyme and glycosyl-enzyme intermediate (an initial and final states) and transition state with the highest energy. Therefore, it becomes possible to explore the ratio of all constants in a simple experiment using the transglycosylation profile.

Analysis of experimental data revealed that the most energetically favourable is the 1,6-linkage, in accordance with its prevalence in nature (stachyose and raffinose saccharides are frequently found in plants)[23]. The lower transition state energy of the 1,3-bond hydrolysis catalysed by this particular enzyme may reflect its preferred use in the processes of recognition and information transfer in living cells. Rare abundance of 1,2-bonds in natural compounds, in our opinion, can be explained by significantly higher energy of this linkage and the highest energy transition state.

Table 4
Kinetic parameters of the TmGalA hydrolysis of galactose-containing substrates

Substrate	K_m, mM	k_{cat}, s^{-1}	k_{cat}/K_m, s mM^{-1}
Melibiose	1.17 ± 0.09	2.33 ± 0.11	1.99 ± 0.25
Raffinose	10.4 ± 0.6	5.0 ± 0.4	0.48 ± 0.07
Stachyose	2.84 ± 0.2	0.53 ± 0.03	0.18 ± 0.02

3. Experimental

3.1. Materials

All chemicals were obtained from Sigma Chemical (St. Louis, USA) or Acros Organics (Geel, Belgium) unless otherwise noted and were used without further purification. *p*-nitrophenyl α-D-galactopyranoside (*p*NPGal) was synthesized from D-galactose as previously described for a glucoside.[20] Galactobiosides with different types of linkages were synthesized and characterized as described in details in Supplemental material (Section S1. Synthesis of galactobiosides).

A plasmid containing the α-galactosidase gene was kindly donated by Prof. R.M. Kelly (North Carolina State University, USA). The α-galactosidase gene from *T. maritima* MSB8 was expressed in *E. coli* BL-21 (DE3) and the recombinant enzyme was purified from cells grown overnight as previously described.[14]

3.2. Synthesis of *p*NP-galactobiosides

All *p*NP-galactobiosides used were synthesized via transglycosylation from *p*NPGal catalysed by *Tm*Gal36A. The transglycosylation reaction was carried out at 60 °C in 50 mM sodium phosphate buffer, pH 7.0. The reaction mixture (3 mL) contained 180 mg (200 mM) of *p*NPGal. The reaction was initiated by the addition of 18 U of the enzyme. The progress of the reaction was monitored by thin layer chromatography as described above. The reaction was stopped by incubating the sample for 10 min in boiling water. To determine the substrate conversion, 5 μL aliquots of the reaction mixture were withdrawn, 10% Na_2CO_3 (3 mL) was added and the

Table 5
Calculated binding free energies for α-galactobioses and natural substrates

Ligand	Position with the lowest binding energy, kJ/M				Average total	$K_b \cdot 10^{-6}$	
	sf	el	en	total			
α-Gal*p*-(1 → 2)-α-Gal*p*	−24.79	−5.19	4.40	−25.58	−25.41	3.79	2.57
α-Gal*p*-(1 → 2)-β-Gal*p*	−23.86	−8.50	4.23	−28.14	−27.05	1.97	
α-Gal*p*-(1 → 3)-α-Gal*p*	−25.41	−14.36	4.31	−35.46	−34.08	0.12	0.067
α-Gal*p*-(1 → 3)-β-Gal*p*	−24.53	−16.70	4.02	−37.22	−36.89	0.04	
α-Gal*p*-(1 → 4)-α-Gal*p*	−23.49	−4.44	3.77	−24.16	−23.53	0.81	4.24
α-Gal*p*-(1 → 4)-β-Gal*p*	−23.57	−4.81	3.94	−24.45	−24.28	5.95	
α-Gal*p*-(1 → 6)-α-Gal*p*	−24.99	−9.50	3.73	−30.77	−28.97	0.91	0.57
α-Gal*p*-(1 → 6)-β-Gal*p*	−23.11	−13.10	4.44	−31.78	−31.02	0.40	
Melibiose: α-Gal*p*-(1 → 6)-α-Glc*p*	−25.54	−14.49	3.81	−36.22	−34.79	0.09	0.78
α-Gal*p*-(1 → 6)-β-Glc*p*	−24.45	−10.13	4.23	−30.35	−28.43	1.13	
Raffinose	−29.35	−7.29	4.86	−31.82	−30.48	0.50	
Stachyose	−38.85	3.52	6.28	−29.06	−26.75	2.21	

sf—hydrophobic energy, el—electrostatic energy, en—entropy loss by amino acid's side chains following the binding with ligand, total—total binding free energy. K_b is binding constant calculated as $K_b = \exp(\Delta G_b/k_B T)$, where k_B is the Boltzmann's constant and T is the temperature.

absorbance at 400 nm in 1 cm path-length cuvette was measured with a Jasco V-560 spectrophotometer.

For separation of the transglycosylation products, the reaction mixture was applied to a Discovery BIO Wide Pore C18 column (250 × 21.2 mm, 10 μm, Supelco) and then eluted with a linear gradient (0–90%) of acetonitrile in water for 180 min at a flow rate of 4 mL/min; the eluent was monitored by absorption at 303 nm. Fractions containing products of transglycosylation were freeze-dried, and compounds were identified by NMR analysis. ^{1}H NMR, ^{1}H–^{13}C HSQC and ^{1}H–^{1}H NOESY measurements were made to identify chemical structures of the *p*NP galactobiosides obtained. The spectra obtained were in a good agreement with the published data.[21]

3.3. Kinetics of transglycosylation reactions followed by in situ proton NMR spectroscopy

Kinetic experiments were performed using a Varian NMR 700 MHz Spectrometer as follows: a tube containing 23 mg or 45 mg of *p*NPGal dissolved in 650 μL of 20 mM deuterium (D_2O) phosphate buffer, pH 7.0, warmed to 50 or 60 °C, placed in the spectrometer, and the magnetic field homogeneity and solvent signal suppression optimized. To suppress the solvent (H_2O) signals, a sequence with water saturation during relaxation or the sequence WET were used. The reaction was initiated by the addition of 100 μL of the *Tm*Gal36A dissolved in the same D_2O phosphate buffer (5.16 U or 11.36 U of the enzyme were used depending on the temperature). To analyse and compare the data obtained, values for the rates in all kinetic experiments were scaled to the lower enzyme concentration. The concentration of each constituent of the reaction mixture was determined by integration of the anomeric non-overlapping proton signals with the following chemical shifts δ: 5.82 for *p*NP1,3diGal (H1), 6.00 for *p*NP1,2diGal (H1), 5.83 for *p*NP1,6diGal (H1), 5.26 and 4.58 for α- and β-galactose (H1), 5.77 for *p*NPGal, 6.91 for *p*NP-OH (*p*-nitrophenol). Data processing has been done using the Varian VNMRJ software, version 3.2C.

3.4. Calculations of kinetic constants and reaction rates

Initial rates for *p*NPGal hydrolysis (V_H^0) and formation of *p*NPdiGals (V_F^i in assumption that $V_H^i = 0$ due to low *p*NPdiGal concentration) were calculated by linear fitting of experimental data from the initial part of the reaction curve treated by Origin 8.0 software (OriginLab Corp., Northampton, MA).

In the case of bell-shaped kinetics curves for the transfer product formation, one can estimate values for the rates of *p*NPdiGals hydrolysis (assuming $V_F^i = 0$ due to low concentration of *p*NPGal) by linear fitting of experimental data from right-hand part of the curve (Fig. 2) treated by Origin. Then, the resulting rate values enable calculation of the ratio of the second order constants for each type of *p*NP-galactobiosides as: $\frac{k_F^i}{k_H^j} = \frac{V_H^i \cdot X_0}{V_H^0 \cdot S_0}$ and $\frac{k_F^i}{k_F^j} = \frac{V_F^i}{V_F^j}$

where V_F^i are initial rates of the *p*NP galactobiosides formation; V_H^i are the initial rates of the *p*NP galactobioside hydrolysis; S_0 is the initial *p*NPGal-substrate concentration; k_F^i and k_F^j are second order rate constants for different *p*NP galactobiosides formation; k_H^i and k_H^j are the rate constants for different *p*NP galactobioside hydrolysis. Indexes *i* and *j* refer to *p*NP galactobiosides with different linkage types.

For ultimate determination of the rate constants k_F^i and k_H^i, least-square fitting of experimental data was made using the programme DYNAFIT[19] by solving the system of differential equations derived from Scheme 1 (Section 2.1, Results and Discussion). For the iterative fitting of *p*NPGal pathway at 50 °C, initial values for rate constants were chosen as: k_3 is approx. equal to k_{cat}, $k_1 = (k_{-1} + k_2)/K_m$), $k_4 = k_1$ and $k_{-4} = k_4/K_I$. For certainty $k_2 > k_3$ and $k_{-1} > k_2$ was assumed. A trial round of fitting included data on decrease of the substrate with fixed values k_3 and k_{-1} and enabled determination of all other constants for the substrate hydrolysis pathway. At the next stage, to estimate initial values for microscopic constants k^i_{-2}, a ratio of initial velocities of hydrolysis and formation of *p*NPdiGals was used as $k^i_{-2} = k_3 \cdot \frac{V_F^i}{V_H^0}$; $V_H{}^0$ is the initial rate of *p*NPGal hydrolysis. At a final round of fitting, values for k^i_1 were fixed at 800 $(\text{mM s})^{-1}$ and second order constants $k_H^i = k_1^i k_2^i/(k^i_{-1} + k^i_{-2})$ and $k_F^i = k^i_{-1} k^i_{-2}/(k^i_{-1} + k^i_{-2})$ were calculated.

3.5. Computer calculations

Spatial structures of α-galactobioses and natural substrates were generated using GLYCAM Carbohydrate Builder (Woods Group. (2005–2014) GLYCAM Web. Complex Carbohydrate Research Center, University of Georgia, Athens, GA. (http://www.glycam.com)). For galactobioses both α- and β-anomeric forms of the reducing galactose residue were constructed. Point charges were assigned to atoms of the substrates in accordance with the GLYCAM06 force field.[24]

A procedure of flexible docking was carried out to identify the modes of binding of α-galactobioses and natural substrates in the active centre of *Tm*Gal36A. The procedure of flexible docking was performed using Molsoft ICM Pro 3.6 package.[25,26] For details see Supplemental material (Section S3. Computer calculations (details)).

3.6. Kinetics of hydrolysis of α-galactobiosides

α-Galactosidase activity towards *p*NPGal was determined at 37 °C in 50 mM sodium acetate buffer, pH 5.0. One unit of the activity was defined as amount of the enzyme releasing 1 μM of nitrophenol from *p*NPGal per min at 37 °C.

The kinetic studies of the *Tm*Gal36A hydrolysis of α-galactobiosides with different glycosidic linkages (1,2diGal, 1,3diGal, 1,4diGal and 1,6diGal) were performed by high performance anion exchange chromatography with pulsed amperometric detection using a Dionex ICS-3000 system (Dionex, Sunnyvale, CA). Reactions were carried out at 37 °C in 50 mM phosphate-citrate buffer, pH 5.0, the total reaction volume was 100 μL. The range of initial substrate concentrations was from 0.009 to 2.4 mM for 1,2diGal, 0.003–0.8 mM for 1,3diGal, 0.03–6.5 mM for 1,4diGal and from 0.005 to 1.7 mM for 1,6diGal. Each reaction was initiated by addition of an appropriate amount of enzyme (0.06–220 mU) and stopped by addition of 10 μL of 0.5 M sodium hydroxide and thorough mixing. The reaction tube was immediately put on ice to avoid spontaneous hydrolysis in the highly alkaline conditions. Aliquots of 10 μL of the reaction mixture were injected on a CarboPac™ analytic column PA10 column (4 × 250 mm; Dionex) mounted on a DIONEX system and thereafter analysed. All reaction products were analysed on the PA10 column at 10 °C and at a flow rate of 0.3 mL/min, using following procedure: 13 min of isocratic elution with 50 mM sodium hydroxide, followed by a linear gradient over 5 min to 80 mM sodium hydroxide and 10 mM sodium acetate. Blank reaction mixtures (without enzyme added) for each reaction were used to correct for spontaneous hydrolysis of the substrate at the high pH of the reaction mixture. The quantification of the hydrolysis products was done by using 5 standards detector was calibrated solutions of known concentration for each sugar over a range of; 0.05–15 mM for the digalactosides, and 0.05–2 mM for galactose. The Dionex system was re-calibrated before and after each analysis using the standards. Peaks were integrated using the software Chromeleon, version 6.8 (Dionex, Sunnyvale, CA). Kinetic parameters were extracted from the experimental curves according to the Michaelis–Menten equation. The curve plot and calculations were made in Origin 8.0 (OriginLab Corp., Northampton, MA).

Measurements of relative hydrolysis rate were made on samples thermostatted at 37 °C in the Dionex sample chamber. The reaction was started by adding the enzyme (0.16–235 mU) and stopped by the injection of the first 10 μL aliquot onto the column equilibrated in 0.05 mM sodium hydroxide. The second 10 μL aliquot of the reaction was injected after one separation method run (27 min). Initial concentrations of substrates were: 4.5 mM (10 K_m) for 1,2diGal, 1.6 mM (26 K_m) for 1,3diGal, 16 mM (8.5 K_m) for 1,3diGal and 1.6 mM (10 K_m) for 1,6diGal.

Competitive inhibition constants for different digalactosides were determined from initial rates of hydrolysis of *p*NPGal (0.016–0.4 mM) in the presence of inhibitor (0.1–10 mM (1,2diGal); 0.02–2 mM (1,3diGal); 0.6–6 mM (1,4diGal); 0.03–0.3 mM (1,6diGal).[27]

3.7. Kinetics of hydrolysis of melibiose, raffinose and stachyose

Purified *Tm*Gal36A (0.13–9.7 mU) was incubated at 37 °C with the substrates, sample volume 50 μL, in 50 mM sodium acetate buffer, pH 5.0. After the reaction was stopped by boiling, liberated glucose was determined by the glucose-oxidase method[9] using melibiose as substrate. Liberated galactose was measured by the Somogyi–Nelson method[28] for the reactions with raffinose and stachyose as substrates. Substrate concentrations were in the range 3–50 mM. The Michaelis–Menten constants K_m and k_{cat} were determined by non-linear least squares fitting of experimental data in Origin 8.0 software.

Acknowledgements

We thank H. Hansson for help with data measurement on regioselectivity in diGal hydrolysis reaction carried out on Dionex equipment. The work was supported by the Russian Foundation for Basic Research (project No. 12-08-00813-a), a personal scholarship from the Swedish Institute to Anna Borisova, and personal fellowship of the Government of Leningrad District, St.Petersburg, Russia to Georgy Rychkov. NMR experiments were carried out using scientific equipment of the Center of Shared Usage «The analytical center of nano- and biotechnologies of Saint Petersburg State Polytechnical University» financially supported by the Ministry of Education and Science of the Russian Federation. Authors thank Prof. Alexey Shavarda for the assistance with mass-spectra recorded at the Core Facilities of the Research Resource Center; 'Molecular and Cell Technologies' at Saint-Petersburg State University. And we thank Christina Payne for her help correcting and proofreading the manuscript.

Supplementary data

Supplementary data associated with this article can be found, in the online version, at http://dx.doi.org/10.1016/j.carres.2014.11.003.

References

1. Bojarová, P.; Kren, V. *Trends Biotechnol.* **2009**, *27*, 199–209.
2. Seeberger, P. H.; Werz, D. B. *Nature* **2007**, *446*, 1046–1051.
3. Shaikh, F. A.; Withers, S. G. *Biochem. Cell Biol.* **2008**, *86*, 169–177.
4. Jahn, M.; Withers, S. G. *Biocatal. Biotrans.* **2003**, *21*, 159–166.
5. Perugino, G.; Trincone, A.; Rossi, M.; Moracci, M. *Trends Biotechnol.* **2004**, *22*, 31–37.
6. Nakai, H.; Baumann, M. J.; Petersen, B. O.; Westphal, Y.; Hachem, M. A.; Dilokpimol, A.; Duus, J. Ø.; Schols, H. A.; Svensson, B. *FEBS J.* **2010**, *277*, 3538–3551.
7. Zhao, H.; Lu, L.; Xiao, M.; Wang, Q.; Lu, Y.; Liu, C.; Wang, P.; Kumagai, H.; Yamamoto, K. *FEMS Microbiol. Lett.* **2008**, *285*, 278–283.
8. Hinz, S. W.; Doeswijk-Voragen, C. H.; Schipperus, R.; Broek, L. A.; Vincken, J. P.; Voragen, A. G. *Biotechnol. Bioeng.* **2006**, *93*, 122–131.
9. Eneyskaya, E. V.; Golubev, A. M.; Kachurin, A. M.; Savel'ev, A. N.; Neustroev, K. N. *Carbohydr. Res.* **1997**, *305*, 83–91.
10. Weignerova, L.; Hunkova, Z.; Kuzma, M.; Kren, V. *J. Mol. Catal. B: Enzym.* **2001**, *11*, 219–224.
11. Takahashi, K.; Hiromi, K.; Ono, S. *J. Biochem.* **1965**, *58*, 255–258.
12. Takahashi, K.; Yoshikawa, Y.; Hiromi, K.; Ono, S. *J. Biochem.* **1965**, *58*, 251–254.
13. Goldberg, R. N.; Bell, D.; Tewari, Y. B.; McLaughlin, M. A. *Biophys. Chem.* **1991**, *40*, 69–76.
14. Comfort, D. A.; Bobrov, K. S.; Ivanen, D. R.; Shabalin, K. A.; Harris, J. M.; Kulminskaya, A. A.; Brumer, H.; Kelly, R. M. *Biochemistry* **2007**, *46*, 3319–3330.
15. Davies, G.; Henrissat, B. *Structure* **1995**, *3*, 853–859.
16. Tewari, Y. B.; Goldberg, R. N. *J. Biol. Chem.* **1989**, *264*, 3966–3971.
17. Jardetzky, T. S.; Seville, M. *Biochemistry* **1988**, *27*, 6758–6763.
18. Cornish-Bowden, A. *Fundamentals of Enzyme Kinetics*, 4th ed.; Wiley-Blackwell: Weinheim, 2013.
19. Kuzmic, P. *Anal. Biochem.* **1996**, *273*, 260–273.
20. Hiromi, K. *Biochem. Biophys. Res.* **1970**, *40*, 1–6.
21. Davies, G. J.; Wilson, K. S.; Henrissat, B. *Biochem. J.* **1997**, *321*, 557–559.
22. Olsson, T. S.; Williams, M. A.; Pitt, W. R.; Ladbury, J. E. *J. Mol. Biol.* **2008**, *384*, 1002–1017.
23. *Storage carbohydrates in vascular plants: Distribution, physiology and metabolism*; Lewis, D. H., Ed.; Cambridge University Press, 1984.
24. Kirschner, K. N.; Yongye, A. B.; Tschampel, S. M.; Gonzalez-Outeirino, J.; Daniels, C. R.; Foley, B. L.; Woods, R. J. *J. Comput. Chem.* **2008**, *29*, 622–655.
25. Abagyan, R.; Totrov, M.; Kuznetsov, D. *J. Comput. Chem.* **1994**, *15*, 488–506.
26. Totrov, M.; Abagyan, R. *Pept. Sci.* **2001**, *60*, 124–133.
27. Dixon, M. *Biochem. J.* **1953**, *55*, 170–171.
28. Nelson, N. *J. Biol. Chem.* **1944**, *153*, 375–380.